JOURNAL OF COMPUTATIONAL PHYSICS 64, 27–55 (1986)

Sensitivity Analysis of Boundary Value Problems: Application to Nonlinear Reaction–Diffusion Systems*

YAKIR REUVEN

Department of Chemistry, Princeton University, Princeton, New Jersey 08540

MITCHELL D. SMOOKE

Department of Mechanical Engineering, Yale University, New Haven, Connecticut 06520

AND

HERSCHEL RABITZ

Department of Chemistry, Princeton University, Princeton, New Jersey 08540

Received July 4, 1984; revised February 25, 1985

A direct and very efficient approach for obtaining sensitivities of two-point boundary value problems solved by Newton's method is studied. The link between the solution method and the sensitivity equations is investigated together with matters of numerical accuracy and efficiency. This approach is employed in the analysis of a model three species, unimolecular, steady-state, premixed laminar flame. The numerical accuracy of the sensitivities is verified and their values are utilized for interpretation of the model results. It is found that parameters associated directly with the temperature play a dominant role. The system's Green's functions relating dependent variables are also controlled strongly by the temperature. In addition, flame speed sensitivities are calculated and shown to be a special class of derived sensitivity coefficients. Finally, some suggestions for the physical interpretation of sensitivities in model analysis are given. © 1986 Academic Press, Inc.

I. INTRODUCTION

Sensitivity analysis is an important numerical tool for the physical investigation and validation of mathematical models [1–5]. At the most basic level it deals with the probing of the relationship between the output information obtained from a model and the input data which includes the model parameters as well as initial and boundary values. When the parameters and their variations are constant in

* Work Supported by the U.S. Department of Energy.

0021-9991/86 $3.00

space and time the *elementary* sensitivities are partial derivatives relating the independent and dependent variables. By applying Legendre transformations it is possible to exchange various independent and dependent variables to calculate derived sensitivities [6, 7]. The full set of all such quantities can be used to address a wide variety of questions about the mathematical modeling of physical processes [1–10]. The importance of the various dependent and independent variables can be assessed and the information gained can be used for further model development or experimental design. Perhaps the simplest application of sensitivity analysis is as a means for estimating inaccuracies in the computed results from mathematical models.

Historically, the major obstacle in obtaining systematically sensitivity information has been the amount of additional computation required for solving the sensitivity equations. Without careful forethought, the solution of the sensitivity equations could exceed the computational effort used in obtaining the model results alone. This can be a serious drawback, especially for models consisting of large systems of differential equations. Continuing effort has gone into alleviating these problems. For example, in the case of initial value problems, an efficient Green's function technique has been developed and successfully implemented for several models [11–13]. The purpose of the present work is to develop and demonstrate efficient methods to calculate sensitivity coefficients for two-point boundary value problems of the form

$$\frac{d^2y}{dx^2} = f\left(x, y, \frac{dy}{dx}; \alpha\right), \qquad a < x < b, \tag{1.1a}$$

with the boundary conditions

$$g_1\left(a, y(a), \frac{dy(a)}{dx}; \alpha\right) = 0, \tag{1.1b}$$

$$g_2\left(b, y(b), \frac{dy(b)}{dx}; \alpha\right) = 0. \tag{1.1c}$$

Here f, y, g_1, and g_2 are N dimensional vectors, generally nonlinear in their arguments, and α is a parameter vector of length M.

Several authors have suggested that, when a numerical procedure based on Newton's method is employed to solve (1.1), the Jacobian matrix can later be used to calculate directly the sensitivity coefficients [14–20]. (This suggestion is not restricted, however, to only boundary value problems.) The present paper examines this concept in detail for the case of two-point boundary value problems. We present a detailed implementation of the method for a simple but interesting model of a one-dimensional flame [21–24]. We also show how to take advantage of the information contained in the sensitivity coefficients and the Green's function matrices to interpret the output results of boundary value problems. Although the present technique does not obtain sensitivities through the Green's functions, the latter

quantities are still calculated since they contain valuable information about the sensitivity of the system's dynamics.

In the next section we describe the global finite difference procedure used in solving the system of equations in (1.1) [25]. In Section III the link between the Newton iteration and the sensitivity coefficients is established. The numerical efficiency of the method used to calculate the sensitivity coefficients is then compared to the alternative method based upon the Green's function approach. In addition, a detailed analysis is presented on the potential errors in the sensitivity coefficients that can result from using numerical Jacobians and inappropriate grid spacings. In Section IV the model problem is discussed, the Green's function matrices are calculated and the numerical accuracy of the sensitivity results is verified. In Section V we systematically calculate the sensitivity coefficients for a steady-state reaction–diffusion model of a premixed laminar flame [21–24]. An extensive model analysis is performed during which the proper usage of the sensitivity information is demonstrated. New physical interpretation for derived sensitivities associated with flame speed analysis is presented in Section VI.

II. Method of Solution

Many problems of physical interest that can be written in the form of (1.1) cannot be solved analytically. As a result, numerical methods are required. Most of the numerical methods that have been used in the solution of two-point boundary value problems can be classified as either initial value (shooting) type methods [26] or global methods such as finite differences or collocation [27, 28]. While initial value methods tend to be easier to implement than global methods, to use them effectively, it is essential that small changes in the initial conditions of the resulting initial value problem result in small changes in the initial value solution. For problems that do not exhibit this behavior, techniques such as multiple shooting [29] and orthonormalization [30] can be used with varying degrees of success. We have found, however, that combustion problems such as burner-stabilized and freely propagating premixed laminar flames are best solved by global methods such as finite differences as opposed to initial value techniques [25]. The subsequent sensitivity algorithm is developed under the assumption that the boundary value problem in (1.1) is solved by an adaptive finite difference procedure.

The first step in this procedure is to obtain a discrete solution of (1.1) on the mesh $\mathcal{M}$

$$\mathcal{M} = \{a = x_0 < x_1 < \cdots < x_m = b\}, \tag{2.1}$$

where $h_j = x_j - x_{j-1}$, $j = 1, 2, \ldots, m$, and $h = \max_{1 \leq j \leq m} h_j$. We approximate spatial derivatives in (1.1) using finite difference expressions. Specifically, we write

$$\frac{d}{dx}\left(a(x)\frac{dg}{dx}\right)_{x_j} \approx \left(\frac{2}{x_{j+1} - x_{j-1}}\right)(a_{j+1/2}\partial g_{j+1} - a_{j-1/2}\partial g_j), \tag{2.2}$$

where we define $g_j = g(x_j)$, $j = 0, 1, \ldots, m$, and

$$g_{j+1/2} = \frac{(g_{j+1} + g_j)}{2}, \qquad j = 0, 1, \ldots, m-1, \tag{2.3}$$

$$\partial g_{j+1} = \frac{(g_{j+1} - g_j)}{h_{j+1}}, \qquad j = 0, 1, \ldots, m-1. \tag{2.4}$$

First derivatives are differenced using the backward difference expressions

$$\left(\frac{dg}{dx}\right)_{x_j} \approx \partial g_j, \qquad j = 1, 2, \ldots, m. \tag{2.5}$$

Newton's Method

By replacing the continuous differential operators in (1.1) by expressions similar to those in (2.2)–(2.5), we convert the problem of finding an analytic solution of (1.1) to one of finding an approximation to this solution at each point of the mesh $\mathcal{M}$. We seek the solution Y_h^* of the nonlinear system of difference equations

$$F(Y_h^*; \alpha) = 0. \tag{2.6}$$

For an initial solution estimate Y^0 that is sufficiently "close" to Y_h^*, the system of equations in (2.6) can be solved by Newton's method. We write

$$Y^{k+1} - Y^k = -\lambda^k J^{-1}(Y^k; \alpha) F(Y^k; \alpha), \qquad k = 0, 1, \ldots, \tag{2.7}$$

where Y^k denotes the kth solution iterate, λ_k the kth damping parameter $(0 < \lambda \leqslant 1)$ and $J(Y^k; \alpha) = \partial F(Y^k; \alpha)/\partial Y$ the Jacobian matrix. We rewrite (2.7) in the form

$$J(Y^k; \alpha)(Y^{k+1} - Y^k) = -\lambda_k F(Y^k; \alpha), \qquad k = 0, 1, \ldots, \tag{2.8}$$

where, for the difference approximations considered, a system of linear block tridiagonal equations must be solved at each iteration for corrections to the previous solution vector. For many problems the cost of forming (either analytically or numerically) and factoring the Jacobian matrix can be a significant part of the cost of the total calculation. In such problems it is natural to consider applying a modified Newton method in which the Jacobian is re-evaluated only periodically. The major problem one faces when applying such a method is how to determine whether the sequence of successive modified Newton iteration steps is converging fast enough. If the rate of convergence is too slow, we return to the full Newton method and make use of new Jacobian information. An error estimate that determines an upper bound for the size of the sequence of modified Newton corrections has been derived in [31]. Improvements in cpu times of up to a factor of two over the full Newton method have been observed with the use of the estimate.

Adaptive Gridding

One of the advantages in using initial value methods in the solution of two-point boundary value problems is the adaptive mesh capability of the initial value solver. Global finite difference methods, however, require that a mesh be determined a priori. Many of the methods that have been used to determine adaptive grids for two-point boundary value problems can be interpreted in terms of equidistributing a positive weight function over a given interval. We say that a mesh $\mathcal{M}$ is equidistributed on the interval $[a, b]$ with respect to the non-negative function W and the constant C if

$$\int_{x_j}^{x_{j+1}} W\,dx = C, \qquad j = 0, 1, \ldots, m-1. \tag{2.9}$$

The major differences in the approaches used center around the choice of the weight function and whether or not the mesh is coupled with the calculation of the dependent solution components. Of the various approaches used, Pereyra and Sewell have equidistributed the local truncation error [32] and White has equidistributed the arclength of the solution [33]. We determine the mesh (see [25]) by employing a weight function that equidistributes the difference in the components of the discrete solution and its gradient between adjacent mesh points. A mesh $\mathcal{M}$ is sought such that

$$\int_{x_j}^{x_{j+1}} \left|\frac{dY_i}{dx}\right| dx \leqslant \delta \left| \max_{a \leqslant x \leqslant b} Y_i - \min_{a \leqslant x \leqslant b} Y_i \right|, \qquad j = 0, 1, \ldots, m-1, \quad i = 1, 2, \ldots, N \tag{2.10}$$

and

$$\int_{x_j}^{x_{j+1}} \left|\frac{d^2 Y_i}{dx^2}\right| dx \leqslant \gamma \left| \max_{a \leqslant x \leqslant b} \frac{dY_i}{dx} - \min_{a \leqslant x \leqslant b} \frac{dY_i}{dx} \right|, \qquad j = 1, 2, \ldots, m-1, \quad i = 1, 2, \ldots, N, \tag{2.11}$$

where δ and γ are small numbers less than one and the maximum and minimum values of Y_i and dY_i/dx are obtained from a converged numerical solution on a previously determined mesh. To avoid the possibility of producing a mesh that is not smoothly varying, the mesh is locally bounded by the relation

$$\frac{1}{A} \leqslant \frac{h_j}{h_{j-1}} \leqslant A, \qquad j = 2, 3, \ldots, m, \tag{2.12}$$

where A is a constant $\geqslant 1$.

In employing the adaptive mesh algorithm, we first solve the boundary value problem on a coarse mesh (4-5 subintervals) and obtain the maximum and minimum values of Y_i and dY_i/dx. The inequalities in (2.10)–(2.12) are then tested

and if any of them is not satisfied, a grid point is inserted at the midpoint of the interval in question. Once a new mesh has been obtained, the previously converged numerical solution is interpolated onto the new mesh. The problem is solved on the new mesh and the process continues until (2.10)–(2.12) are satisfied.

III. Sensitivity Analysis

The goal is now to predict the effect of the variation of the parameter vector α on the dependent variable Y. The quantities of interest are the first order sensitivity coefficients $\partial Y/\partial \alpha_k$, $k = 1, 2,..., M$. The appropriate equations for these quantities can be derived by differentiating (2.6) with respect to α_k. We have

$$\frac{d}{d\alpha_k}(F(Y;\alpha)) = \frac{\partial F}{\partial Y}\frac{\partial Y}{\partial \alpha_k} + \frac{\partial F}{\partial \alpha_k} = 0, \qquad k = 1, 2,..., M, \tag{3.1}$$

where we have omitted the subscript h and superscript *. Recalling that the Jacobian matrix is given by $J = \partial F/\partial Y$, we have

$$J\frac{\partial Y}{\partial \alpha_k} = -\frac{\partial F}{\partial \alpha_k}, \qquad k = 1, 2,..., M. \tag{3.2}$$

We remark that, although Eq. (3.2) can be solved at any level of the Newton iteration and at any level of grid refinement, we solve it on the finest grid with the last Jacobian formed. It is only at this stage of the calculation that the numerical solution has been resolved with sufficient accuracy to represent the analytic solution. Equations (3.1) and (3.2) can also be arrived at by differentiating (1.1) followed by discretization. In principle, the differential equation for $\partial Y/\partial \alpha_k$ should be discretized on its *own* mesh independent of that used in solving (2.6). However, proceeding with the mesh chosen from (2.6) has an enormous advantage from the standpoint of computational efficiency. From another perspective, (3.1) is the *exact* sensitivity equation associated with the discretized approximate result in (2.6). Various aspects of error analysis will be explored in more detail below.

First-Order Sensitivity Coefficients and Green's Functions

We point out that although the original boundary value problem can be nonlinear, the sensitivity equations in (3.2) are linear. In principle, we can apply the Green's function method to obtain a solution to (3.2). While we do not advocate such a procedure, the Green's function does, however, contain valuable information on system sensitivity. The Green's function satisfies the equation

$$JG = -\Delta, \tag{3.3}$$

where the diagonal matrix Δ can be written in terms of $N \times N$ diagonal blocks δ_j, $j = 1, 2,..., m$. To insure that the Green's function vanishes at the boundaries, the

diagonal blocks corresponding to $j=1$ and $j=m$ are set identically to zero. The nonzero diagonal entries of the remaining blocks $j=2, 3,..., m-1$ are given by

$$(\delta_j)_{kk} = \frac{2}{h_j + h_{j+1}}, \qquad k = 1, 2,..., N. \tag{3.4}$$

With the definition in (3.4), we can obtain G by solving the linear system $JG = -\Delta$. Assuming the Jacobian has been factored, formation of G is accomplished by performing Nm back substitutions with a different column of Δ as the right-hand side. As a result of the difference approximations used, the Jacobian matrix can be written in block tridiagonal form. Its factorization requires approximately $7N^3m/3$ additions and multiplications. To perform a back substitution requires approximately $3N^2m$ additions and multiplications. Hence, to form G we require

$$\text{Number of Operations} = \frac{7N^3m}{3} + 3N^3m^2. \tag{3.5}$$

If one actually forms G as described above, the first order sensitivity coefficients can be obtained by forming

$$\frac{\partial Y}{\partial \alpha_k} = G\frac{\partial F}{\partial \alpha_k}, \qquad k = 1, 2,..., M, \tag{3.6}$$

at an additional cost of $Nm-1$ additions and Nm multiplications.

In the current application, however, the Jacobian matrix is formed and factored into its LU decomposition as a result of the Newton iteration. The first-order sensitivity coefficients are found by solving (3.2) at a cost of $3N^2m$ additions and multiplications per coefficient.

First-Order Sensitivity Coefficients and Numerical Jacobians

In practice, the Jacobian matrix in (2.8) is computed numerically. Providing the error introduced by forming a numerical approximation to J is not too "large," Newton's method applied to (2.6) can be shown to converge for a suitably good initial guess [34]. For our purposes, we want to investigate the error in the first-order sensitivity coefficients that is introduced as a result of using an approximation to J. The numerical Jacobian $\tilde{J}$ may be written as

$$\tilde{J} = J + \delta J, \tag{3.7}$$

where δJ is a perturbation matrix of the analytic Jacobian J. Since we form the quantities $\partial F/\partial \alpha_k$ numerically, we can write

$$\frac{\partial \tilde{F}}{\partial \alpha_k} = \frac{\partial F}{\partial \alpha_k} + \delta\frac{\partial F}{\partial \alpha_k}, \tag{3.8}$$

where $\delta(\partial F/\partial \alpha_k)$ is a perturbation of the analytic inhomogeneity $\partial F/\partial \alpha_k$. Introducing (3.7) and (3.8) into (3.2) produces

$$(J+\delta J)\left(\frac{\partial Y}{\partial \alpha_k}+\delta\frac{\partial Y}{\partial \alpha_k}\right)=-\left(\frac{\partial F}{\partial \alpha_k}+\delta\frac{\partial F}{\partial \alpha_k}\right), \qquad k=1, 2,..., M, \tag{3.9}$$

where $\delta(\partial Y/\partial \alpha_k)$ is the perturbation (error) in the kth first-order sensitivity coefficient. From standard linear perturbation theory, it follows that

$$\frac{\left\|\delta\dfrac{\partial Y}{\partial \alpha_k}\right\|}{\left\|\dfrac{\partial Y}{\partial \alpha_k}\right\|}\leqslant\frac{\kappa(J)}{1-\kappa(J)\dfrac{\|\delta J\|}{\|J\|}}\left[\frac{\|\delta J\|}{\|J\|}+\frac{\left\|\delta\dfrac{\partial F}{\partial \alpha_k}\right\|}{\left\|\dfrac{\partial F}{\partial \alpha_k}\right\|}\right], \tag{3.10}$$

for some norm $\|\cdot\|$ and where $\kappa(J)=\|J\|\,\|J^{-1}\|$ is the condition number of the Jacobian. If $\kappa(J)$ is large, then small relative perturbations in J and $\partial F/\partial \alpha_k$ will produce large relative perturbations in $\partial Y/\partial \alpha_k$. In addition, if we let δY_j denote the perturbation of the jth component of Y, then Taylor series arguments can be used to show

$$\|\delta J\|\leqslant\frac{1}{2}\|\delta Y\|\left\|\frac{\partial^2 F}{\partial Y^2}\right\|. \tag{3.11}$$

If we combine (3.11) with (3.10), we see that large relative perturbations in the first-order sensitivity coefficients result from: (1) a high condition number of the Jacobian and/or (2) large second derivatives of the nonlinear function, and/or (3) large perturbations of the dependent solution vector used in evaluating $\tilde{J}$.

First-Order Sensitivity Coefficients and Adaptive Grids

We have concentrated most of our discussion on the determination of the first-order sensitivities by utilizing the numerical Jacobian on the finest grid. The analysis has focused on the discretization of the original equations and the subsequent solution of the nonlinear difference equations by Newton's method. The process could equally be applied in reverse, as indicated earlier—linearize the original equations and then discretize the differential operators. In this section we compare the effects of applying each procedure in the calculation of the first-order sensitivity coefficients. To facilitate a discussion of these ideas, consider the scalar analogue of (1.1) with Dirichlet boundary conditions

$$\begin{aligned}\frac{d^2y}{dx^2}&=f\left(x, y, \frac{dy}{dx}; \alpha\right), \qquad a<x<b,\\ y(a)&=y_a,\\ y(b)&=y_b,\end{aligned} \tag{3.12}$$

where α is a scalar parameter. If we differentiate (3.12) with respect to α and denote primes as differentiation with respect to x, we have

$$\frac{d^2}{dx^2}\left(\frac{\partial y}{\partial \alpha}\right)=\frac{\partial f}{\partial y}\left(\frac{\partial y}{\partial \alpha}\right)+\frac{\partial f}{\partial y'}\frac{d}{dx}\left(\frac{\partial y}{\partial \alpha}\right)+\frac{\partial f}{\partial \alpha}. \tag{3.13}$$

With the definition $z=\partial y/\partial \alpha$ we have

$$z''=\frac{\partial f}{\partial y'}z'+\frac{\partial f}{\partial y}z+\frac{\partial f}{\partial \alpha}, \tag{3.14}$$

which is a linear second-order differential equation for the first order sensitivity coefficient. If the differential operators in (3.14) are discretized with expressions similar to those in (2.2)–(2.5), then it can be shown that the discrete equations obtained are identical to those that result from applying to (3.12) the procedure that led to (3.2)—providing the grids used are the same in both calculations. We point out that in solving (3.12) we would use an adaptive finite difference procedure. This same approach could be used in solving (3.14). In practice due to the derivative terms of f with respect to y and y', (3.12) and (3.14) would be solved simultaneously. There is no guarantee, however, that the grids used in both calculations would be identical. In the solution of (3.14) the location of the grid points would be based upon properties of the first-order sensitivity coefficients. The grids can differ since the first-order sensitivity coefficients may have regions of high spatial activity in regions where the solution y is smooth and vice versa. Two questions arise. First, how do the different mesh spacings affect the first-order sensitivity coefficients and, second, what procedure could be used to guarantee that the proper mesh is used even though we determine the sensitivity coefficients from (3.2)?

An analysis of the effect of different mesh spacings based upon general nonuniform grids is quite difficult. Instead, we consider the solution of (3.12) and (3.14) on uniform grids with a different number of grid points and with first derivatives approximated by centered difference expressions. We assume that the solution of (3.14) has been obtained to a desired level of accuracy on a grid with mesh spacing h. In addition, we assume that the solution of (3.12) has been obtained on a coarser grid, with mesh spacing $(1+k)\,h$ for an integer k. This situation is analogous to the case in which the grid for (3.12) is not as refined as the grid for (3.14) in regions where the spatial activity of $\partial y/\partial \alpha$ is high.

One can show (see [28]) that under appropriate smoothness assumptions, there exists a function $e(x)$ independent of the mesh spacing h such that the error in the numerical solution of (3.14) has the form

$$z(x_j)-z_j=h^2e(x_j)+O(h^4), \qquad 0\leqslant j\leqslant\frac{b-a}{h}, \tag{3.15}$$

where z_j is the numerical approximation to $\partial y/\partial\alpha$ at x_j. Similarly, one can show

$$\frac{\partial y(x_j)}{\partial\alpha}-\frac{\partial y_j}{\partial\alpha}=(1+k)^2\,h^2 e(x_j)+O((1+k)^4\,h^4),\qquad 0\leqslant j\leqslant\frac{b-a}{(1+k)\,h}. \tag{3.16}$$

If (3.16) is subtracted from (3.15), then for a point common to both meshes, we find

$$\frac{\partial y_j}{\partial\alpha}-z_j=k(2+k)\,h^2 e(x_j)+O(h^4). \tag{3.17}$$

We observe that the sensitivity coefficient determined directly from (3.12) is equal to the sensitivity coefficient determined from (3.14) plus a correction term that is $O(h^2)$. The coefficient of this term depends upon the size of the mesh spacing used in the coarser grid calculation.

After obtaining a solution to (3.2), the equidistribution principle (2.10)–(2.12) could be applied to the calculated sensitivity coefficients $\partial y/\partial\alpha_k$. In this way we can determine whether the mesh used in the solution of (1.1) has to be refined to solve again for y and $\partial y/\partial\alpha_k$. This procedure would be terminated when the calculated values of $\partial y/\partial\alpha_k$ satisfy (2.10)–(2.12). Although such a procedure could add significantly to the cost of the original problem, it would assure accurate solutions and accurate sensitivity coefficients. In practice, many problems will likely be of the type where the sensitivity functions show strong spatial behavior in the same regions as that for the original solution. An exception to this "rule" would occur for singular perturbation (sensitivity) problems. Extensive numerical calculations on a variety of systems will be helpful in finally assessing these issues.

IV. Model System

The computations presented in this section serve the dual purpose of testing some of the numerical matters raised in the last section, as well as providing an interesting physical example for analysis. A model flame system will be used to bring out both issues. Special emphasis will be given to the physical interpretation of the sensitivity coefficients and the Green's function matrices. A simple, two-stage, unimolecular, one-dimensional flame represented by the mechanism

$$C_r\rightarrow C_i\rightarrow C_p$$

is chosen as the illustrative model.

After utilizing the coordinate transformations and nondimensionalizations discussed in [21–24], the system can be described, under steady-state conditions, by the following nonlinear two-point boundary value problem

$$M_0\frac{dC_r}{dx}=\frac{1}{Le_r}\frac{d^2C_r}{dx^2}-k_{ri}C_r\exp(-E_r/T), \tag{4.1}$$

$$M_0 \frac{dC_i}{dx} = \frac{1}{Le_i} \frac{d^2C_i}{dx^2} + k_{ri} C_r \exp(-E_r/T) - k_{ip} C_i \exp(-E_i/T), \tag{4.2}$$

$$M_0 \frac{dT}{dx} = \frac{d^2T}{dx^2} + k_{ri}(h_r - h_i)\, C_r \exp(-E_r/T) + k_{ip} h_i C_i \exp(-E_i/T), \tag{4.3}$$

on the domain $0 \leqslant x < \infty$. The boundary conditions at $x = 0$ are given by

$$C_r - \frac{1}{M_0 Le_r} \frac{dC_r}{dx} = \varepsilon_r, \tag{4.4}$$

$$C_i - \frac{1}{M_0 Le_i} \frac{dC_i}{dx} = \varepsilon_i, \tag{4.5}$$

$$T = T_0, \tag{4.6}$$

and as $x \to \infty$ by

$$\frac{dC_r}{dx} = \frac{dC_i}{dx} = \frac{dT}{dx} = 0. \tag{4.7}$$

In practice the solution domain is truncated at a large value of $x = L$ such that the zero gradient boundary conditions are "satisfied." For the calculations presented in this section, we set $L = 10$.

In the above equations T denotes the temperature and C_r and C_i the mass fraction concentrations of the reactant and intermediate, respectively. The product concentration C_p is determined from conservation of mass. We have

$$C_p = 1.0 - C_r - C_i. \tag{4.8}$$

Values for the pre-exponential constants k_{ri}, k_{ip}, the activation energies E_r, E_i, the Lewis numbers Le_r, Le_i, the specific enthalpy differences between the reactant and product h_r and the intermediate and product h_i, the mass flux fractions ε_r and ε_i,

TABLE I

Parameters for the Model Flame System

Parameter	Value
k_{ri}	5.0×10^8
k_{ip}	1.0×10^2
E_r	80.0
E_i	10.0
Le_r	0.75
Le_i	1.25
h_r	4.4
h_i	4.5
ε_r	1.0
ε_i	0.0
T_0	1.25
M_0	0.985

the burner temperature T_0 as well as the initial mixture flow rate M_0 are listed in Table I. Quantities such as the thermal conductivity and the specific heat capacity do not appear explicitly in the model because they are contained in the other non-dimensionalized variables.

We point out that asymptotic analyses of this reaction-diffusion system have been performed [21–24] and resulting analytical expressions for the flame velocity and species concentrations have been obained for several values of activation energies, pre-exponential constants and Lewis numbers. Although the three-species model is rather schematic and has limited ability to account for the behavior of real complex flames, it still contains terms that represent the main processes occurring in larger, many-species, reaction–diffusion systems.

Model Verification

The system of equations (4.1)–(4.8) was solved numerically using the adaptive finite difference method described in Section II. Typical solution curves are presented in Fig. 1a. It can be seen that, for the parameter values listed in Table I, the concentration of the intermediate remains small along the entire reaction region with a peak value an order of magnitude less than the initial value of the reactant. Another observation is that, for the nondimensionalized flame speed $M_0 = 0.985$, the flame is practically adiabatic as there are no significant changes in the species and the temperature near the burner from their prescribed boundary values. Before reaching the other boundary, the reaction is effectively completed and the species and the temperature assume their constant steady-state values.

The nonlinearities in Eqs. (4.1)–(4.3) arise only via the exponential temperature dependence of the reaction terms. Hence, by enforcing a constant temperature (thus replacing Eq. (4.3) with $T = T_{\text{known}}$), the system becomes linear. In such a case an analytical solution can be obtained to Eqs. (4.1) and (4.2). Analytical solutions for

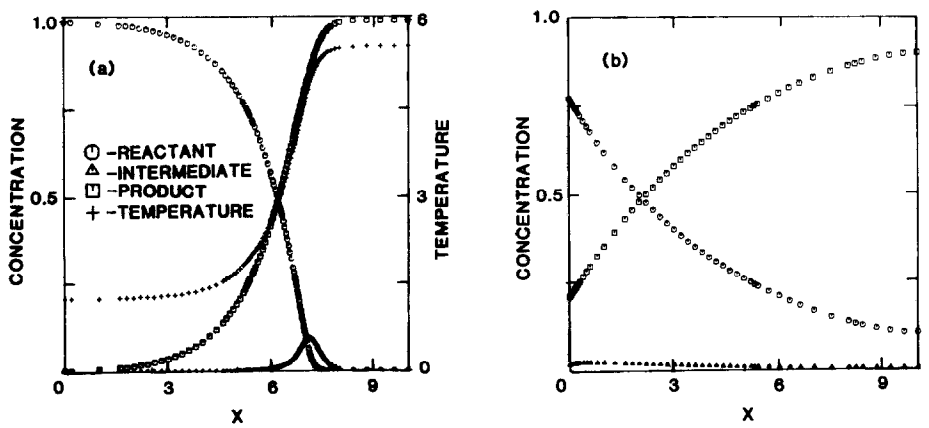

FIG. 1. Solution of the three species model with predetermined flame speed and $k_{ip} = 1.0 \times 10^2$. (a) Variable temperature. (b) the temperature is forced to be constant with $T = 3.75$ (not shown). The right-hand scale refers to the temperature values.

a similar model, but without the convective terms, were employed first to test and verify the accuracy of the numerical solutions, the sensitivity coefficients and the various Green's function matrices.

The solution profiles obtained for constant temperature, $T = 3.75$, are illustrated in Fig. 1b. All other parameter values are identical to those of the nonlinear solution in Fig. 1a. A system of this type could be achieved effectively by adding a large amount of inert diluent in the flow. Appreciable amounts of product appear at the burner and the intermediate also peaks very close to it. The flame "region" is much larger, and the reaction is not completed at the second boundary. The numerical results obtained for the sensitivities in the linear case were in good agreement with the sensitivity coefficients obtained analytically from the solution of a system of equations similar to (3.14).

An interesting and somewhat surprising behavior of the sensitivity of the intermediate with respect to variations in k_{ri} in the linearized system can be seen in Fig. 2. From Eq. (4.2) it is obvious that the reactant causes an increase in the concentration of the intermediate. This is reflected by a positive sensitivity curve for the intermediate in the region where the concentration of the reactant is still large (see Fig. 1b). However, where the amount of the reactant is reduced considerably ($x \geqslant 4.5$), a further increase in k_{ri} causes a large negative response in the intermediate concentration. At this point in the flow the depletion term in Eq. (4.2) becomes dominant and increasing k_{ri} just reinforces this effect. The behavior of the sensitivity results for the reactant and product are in clear accord with this view.

Besides serving as a case for easy numerical evaluation, the linear system provides useful insight. In particular, the behavior demonstrated by the sensitivity coefficients and the Green's function matrices can reveal whether, under appropriate conditions, the nonlinear system or parts of it exhibit behavior that is approximately linear. These points of comparison will be examined below.

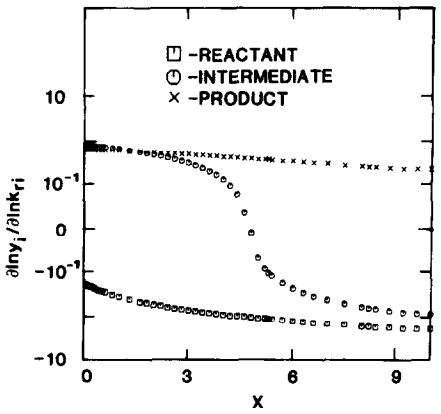

FIG. 2. Normalized first-order sensitivity coefficients with respect to k_{ri} for the solution with constant temperature.

Green's Function Behavior

The Green's function matrices contain global information about the stability of the system and its response to various types of perturbations in the entire region of interest. Furthermore, of all the possible sensitivities in a problem (besides those with respect to laboratory control parameters) the Green's function elements are unique in that they, in principle, can be measured. The Green's function matrices were obtained from a numerical solution of the algebraic equations (3.2) and (3.3) using the Jacobian from the last step of the Newton iteration.

We consider first the linear system at constant temperature. An example is shown in Fig. 3 for $G_{ir}(x, x')$ which is the response surface of the intermediate at x to a disturbance of the reactant at x'. It can be seen that the surface is almost structureless except for a small positive response along the main diagonal which is the region where x is in the proximity of x'. This behavior is typical of a linearly stable system: namely, a small and localized response to a perturbation over the entire solution region. The positive response is expected in this case since the reactant acts as a source for the production of the intermediate (see Eq. (4.2)). Similar behavior was observed for the other Green's function surfaces in the linear case, although the response along the diagonal $x = x'$ is somewhat larger when the same species is perturbed (i.e., consider G_{ii} (x, x')). The surface for $G_{ri}(x, x')$ is, of course, zero since the reactant is not affected by any other dependent variable in the linear case.

If we consider the nonlinear flame shown in Fig. 1a, it is interesting to examine first the Green's function matrices shown in Fig. 4. Comparison with Fig. 3 reveals that the stability characteristics of the system are changed dramatically. Generally, the response to perturbations becomes larger and they vary significantly in the flame region. The magnitude of the response no longer depends on the distance from the perturbation point, but on the distance from the flame region. The responses are largest in the region where the flame occurs. As a result, the response surfaces are no longer diagonally ($x \sim x'$) dominant, but are rather strong functions of the response point x and weak functions of the disturbance point x'. Another com-

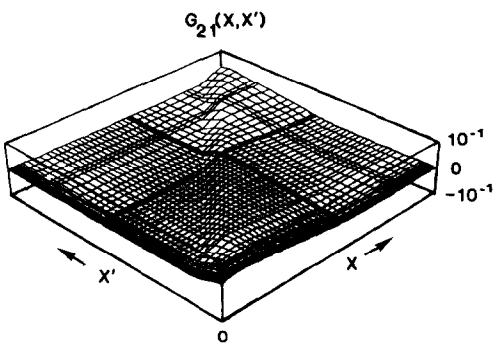

FIG. 3. The Green's function matrix $G_{ir}(x, x')$ for the solution with constant temperature. The vertical scale is logarithmic.

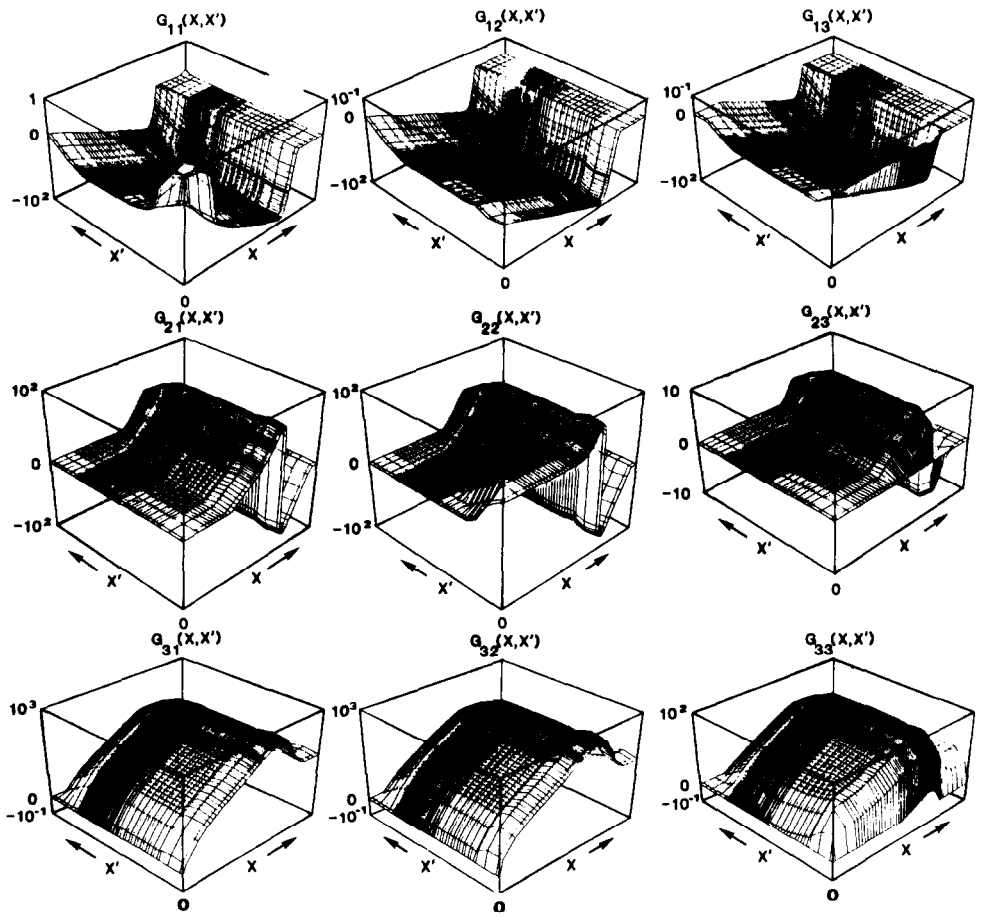

FIG. 4. The Green's function matrices for the variable temperature system with predetermined flame speed and $k_{ip} = 1.0 \times 10^2$. The subscripts refer to (1) reactant, (2) intermediate, and (3) temperature. The vertical scales are logarithmic.

mon feature of the response surfaces is that their structure is quite similar when responses of the same dependent variable are considered—no matter which variable is causing the perturbation.

We point out that the reactant responds negatively to any positive perturbation

positive response. Any positive change in the reacting species or in the temperature increases the reaction activity of this exothermic system, thereby increasing the temperature.

The Green's function matrices for the intermediate indicate mainly that the shape of the intermediate concentration curve will be affected in such a way that its

maximum will be shifted closer to the burner if any of the species or the temperature is increased. This again may be understood in a similar fashion to the discussion above.

V. Sensitivity Coefficients and Analysis

The sensitivities (other than the Green's functions) are presented in this paper as normalized quantities $\partial \ln y/\partial \ln \alpha_k$. Here y stands for a dependent variable and α_k is a specific parameter in the equations or boundary conditions. In this way, relative variations are considered and this allows for a comparison between different sensitivity coefficients. In cases where the nominal value of the parameter is zero, seminormalized sensitivities $\partial \ln y/\partial \alpha_k$ are calculated. The results for the sensitivity coefficients are shown in semilogarithmic plots. To handle the plus and minus signs, as well as to eliminate the effect of very small sensitivity values on the logarithmic scale of the plots, all the normalized sensitivity results of magnitude less than or equal to 10^{-2} were set equal to zero. Thus only sensitivities larger than one percent are considered.

Boundary Condition Sensitivities

Since the temperature is the quantity through which all the components of the nonlinear system are coupled, the characteristics of its behavior have a major role in determining the final outcomes. The important feature of the temperature is its participation in the exponential terms of the model which results in a dominant influence on the kinetics of the flame. The sensitivity coefficients of the temperature with respect to the boundary conditions are shown in Fig. 5a. All the sensitivity

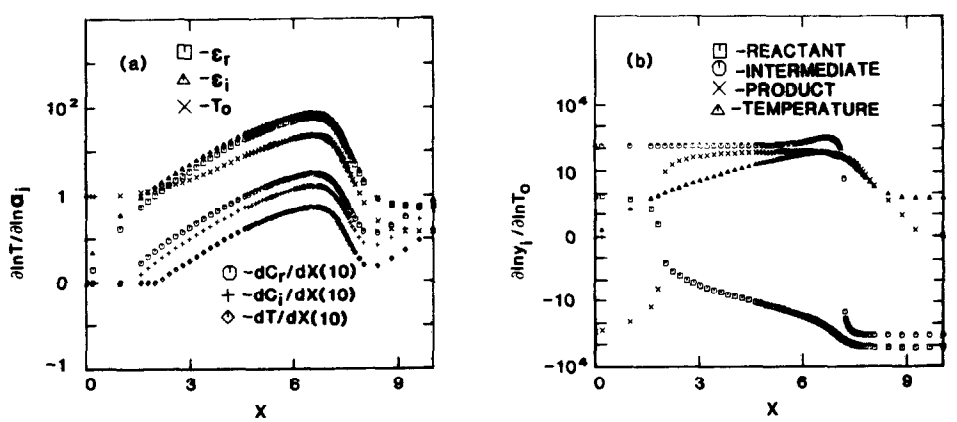

FIG. 5. Normalized first-order sensitivity coefficients with respect to the boundary values for the variable temperature system with predetermined flame speed and $k_{ip} = 1.0 \times 10^2$. (a) The sensitivity of the temperature with respect to all boundary values. (b) the sensitivities of the species and the temperature with respect to the boundary value of the temperature at $x = 0$.

curves in this figure behave similarly as a function of position and the patterns resemble those observed for the temperature Green's function surfaces (see Fig. 4). This may be understood from the behavior of Fig. 4 and the role of G in Eq. (3.6). The only difference is in the magnitude of the sensitivities. Two distinct groups can be identified among the curves. The one with the larger sensitivity values belongs to the boundary conditions at $x = 0$, whereas the less sensitive curves are for the downstream boundary. Note also that the sensitivity coefficients are positive along the entire system region. This indicates that increasing the value of any boundary condition will cause a positive change in the temperature, especially in the flame region. Increasing the species concentrations at the boundaries will enhance the reaction activities inside the system region. In addition, since the reaction is exothermic, there will be an increase in the temperature.

Species sensitivity coefficients with respect to the boundary value of the temperature at $x = 0$ can be seen in Fig. 5b. Note again that the main structural changes in the curves occur in the flame region. It can be seen that an increase in the temperature at $x = 0$ tends to shift the position of the intermediate peak closer to the burner. An increase in the temperature results in an increase in the magnitude of all the reaction terms in the system. As a result, the reactant concentration decreases and the intermediate concentration increases in the region in which the positive reaction term dominates equation (4.2). This activity will, of course, increase the amount of product which is reflected in its positive sensitivity profile in Fig. 5b.

System Parameter Sensitivities

Sensitivity coefficients for the solution of the nonlinear system with respect to the system parameters are presented in Figs. 6–8. Figure 6 illustrates the sensitivity coefficients of the temperature with respect to all the parameters and those for the

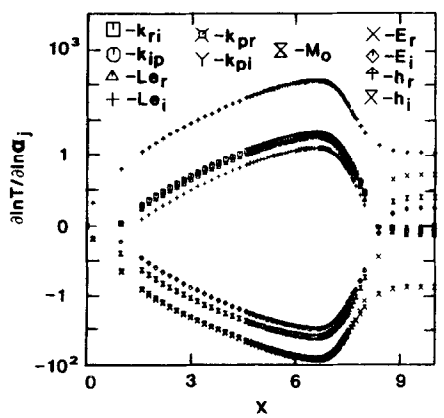

FIG. 6. Normalized first-order sensitivity coefficients of the temperature with respect to the system parameters for the variable temperature model with predetermined flame speed and $k_{ip} = 1.0 \times 10^2$.

intermediate are shown in Fig. 7. Inspection of Fig. 6 reveals that the temperature is most sensitive to variations in the specific enthalpies. The resultant variations in the temperature are significantly larger in the region of the flame. The increase on the temperature when h_r is increased results from its appearance in a positive term in the energy equation (4.3). Similar variations in h_i result in an almost equivalent decrease in the temperature. Since h_i participates in both a positive term and a negative term in the same equation, the above sensitivity behavior implies that the contribution from the negative term dominates.

Comparison between Figs. 6 and 7, along with additional sensitivity results not shown here, reveals that the intermediate is relatively more sensitive to variations in the specific enthalpies than the temperature, even though these parameters do not participate directly in the equation for the intermediate. This is another demonstration of the exponential nonlinearity of the temperature. Small variations in the temperature are magnified producing large variations in the intermediate.

The increase in the temperature when k_{ri} is perturbed is, at first sight, unexpected. The reaction $C_r \rightarrow C_i$ is endothermic according to the values selected for the specific enthalpies. However, an increase in k_{ri} also results in a decrease of the reactant concentration (see Eq. (4.1)) which, in turn, causes a decrease in the effect of the endothermic term in the temperature equation. In addition, the intermediate concentration is increased and, hence, a respective increase is expected in the overall exothermicity of the flame system. It appears that the two indirect effects described above are more important than the direct effect that k_{ri} has on the temperature. The positive change of the temperature when k_{ip} is increased suggests that in this case the direct effect has a larger influence than the opposing indirect effect of k_{ip} through a decrease in the amount of the intermediate. Indeed, in Fig. 7 it is clear that these effects can even compete at positions beyond the flame region.

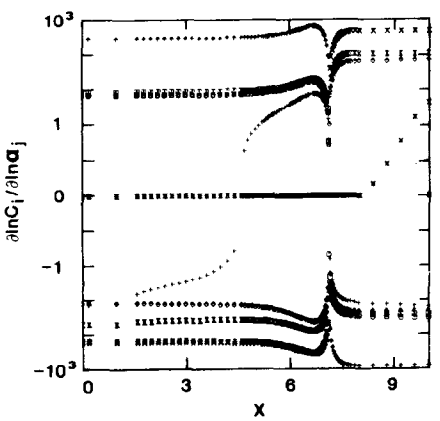

FIG. 7. Normalized first-order sensitivity coefficients of the intermediate with respect to the system parameters for the variable temperature model with predetermined flame speed and $k_{ip} = 1.0 \times 10^2$. The legend is the same as in Fig. 6.

In Fig. 6 and 7 we also observe the contribution of the sensitivities with respect to reverse rate constants of the product. The product is essentially the only species remaining near the hot boundary and, therefore, its rate terms should be dominant in this region. This is reflected by an increased sensitivity to its rate terms (k_{pi} and k_{pr}), although the nominal value of the respective rate constants is zero.

In Fig. 8 the sensitivities with respect to the rate constant k_{ri} for passage from reactant to intermediate are presented. Comparison with Fig. 5b reveals again the similar effect that variations of each parameter have on the dependent variables for the parameter values selected here. The similarity of the curves in both figures shows again that the effect of parameter variations is channeled through the temperature in the present model. It is interesting to compare Fig. 8 with Fig. 2 which presents the same sensitivities for the linear (constant temperature) case. Note the smaller values that the sensitivity coefficients assume in the linear system. This reflects its increased stability. Another fact that should be mentioned in this context is that, although the general patterns of the sensitivity coefficients for the intermediate look similar, they arise due to *different* reasons. The sensitivity coefficient of k_{ri} in Fig. 2 reflects the direct effect that this rate constant has in the equation for the intermediate. In the nonlinear case the same sensitivity coefficient reflects the dominant indirect effect that this rate constant has through the temperature on the overall rate for the intermediate concentration. This analysis is supported by the observation that the sensitivity coefficient in the nonlinear case changes sign at the position where the intermediate peaks. The change of sign in the linear case takes place in an entirely different position (see also Figs. 1a and 1b).

The numerical results described so far were obtained for a relatively small rate constant for depletion of the intermediate, $k_{ip} = 1.0 \times 10^2$. The value was chosen to ensure that a "significant amount" of the intermediate could be accumulated at

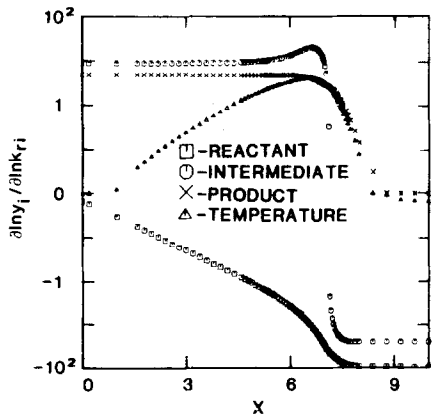

FIG. 8. Normalized first-order sensitivity coefficients of the system variables with respect to k_{ri} for the variable temperature model with predetermined flame speed and $k_{ip} = 1.0 \times 10^2$.

some region of the flame. Another interesting case for which a similar analysis was carried out was for $k_{ip} = 1.0 \times 10^7$. From the results for the species and the temperature profiles (not shown here), it was found that the concentration of the intermediate was practically zero along the entire flow region. Another difference from the previous case is that a higher flow speed ($M_0 = 1.25$) was required to achieve adiabatic conditions. The flame was also confined to a narrower region and the temperature rise was steeper.

For the most part, the sensitivity coefficients in the case $k_{ip} = 1.0 \times 10^7$ (not shown) display behavior similar to the respective sensitivity coefficients in the previous case. Variations in the sensitivity curves are in accordance with the different flame region. The fact that the amount of the intermediate is very small causes a respective reduction in the rate terms in which it participates. As a result, the temperature and therefore the reactant are no longer sensitive to variations of the intermediate parameter. Moreover, the direct effect that a variation in k_{ip} has on the intermediate dominates the indirect effect it has through the temperature. This fact is manifested by the sensitivity coefficient of the intermediate with respect to k_{ip} which is now negative along the entire system region. This behavior is completely different from the same function in the case discussed previously in Fig. 7.

The activation energies participate in the same rate terms in the system of equations as the respective rate constants. However, since their effect is exponential and opposite to the effect of the rate constants, the response of the temperature to activation energy variations is more pronounced and opposite to the response when the rate constants are perturbed. In addition, by dividing the energy equation with respect to the flame speed, it can be observed immediately that increasing the value of M_0 will reduce the overall rise of the temperature and this is reflected by the negative values of the corresponding sensitivity function.

Constrained Temperature Sensitivities

The last case for which the solutions and the sensitivity coefficients are calculated is an extension of the system presented in Eqs. (4.1)–(4.8). In the previous system the flame speed M_0 was treated as a specified parameter. In many cases this quantity is, in fact, not known and must be determined from the given system of equations and the boundary conditions. This problem can be approached by extending the system to a generalized eigenvalue problem with the flame speed determined by the approach considered in [35]. To implement this procedure, the temperature is constrained at a point inside the solution domain in addition to the boundary value it has at the cold burner. The flame speed that is consistent with such a temperature constraint can then be determined by adding to (4.1)–(4.8) the following trivial differential equation and boundary condition

$$\frac{dM_0}{dx} = 0, \qquad T(x^*) = T^*. \tag{5.1}$$

This corresponds mathematically to changing the identification of the flame speed

from a parameter to a dependent variable (see also the next section).[1] The new augmented system of equations can be solved by the method described in Section II.

In the system under consideration, Eqs. (4.1)–(4.8) were solved with the temperature constrained at $x^* = 1.6$. The temperature value was taken from the temperature at x^* shown in Fig. 1a. Solution profiles identical to those displayed in Fig. 1a were obtained and a similar value for the flame speed ($M_0 = 0.98$) was calculated. The results obtained for the sensitivity coefficients, however, differ considerably. It is illuminating to see how fixing T^* at x^* affects the other system sensitivities. A representative example is shown in Fig. 9 in which the sensitivity coefficients of the reactant and the intermediate, with respect to k_{ip}, are displayed for both cases. Note that the two systems show different sensitivities near T^* and the system with T fixed near x^* generally becomes less sensitive in that region. The results for the sensitivity coefficients, however, are similar in the flame region and near the hot boundary. Fixing the temperature value at an interior point reduces the sensitivity of the temperature in the vicinity of that point to parameter variations. This causes a respective decrease in the sensitivity of the species.

Interesting behavior is displayed by the sensitivity coefficient of the intermediate with respect to k_{ip}. In the region between the cold boundary and the position at which the temperature is prescribed, a positive change in k_{ip} now causes a decrease in the intermediate concentration. This is the direct effect that we expect k_{ip} to have on C_i (see Eq. (4.2)). Since the temperature is not sensitive to variations in k_{ip} in this region, the indirect effect of perturbations in k_{ip} through a respective perturbation in the temperature is negligible. Only when one moves further away from the

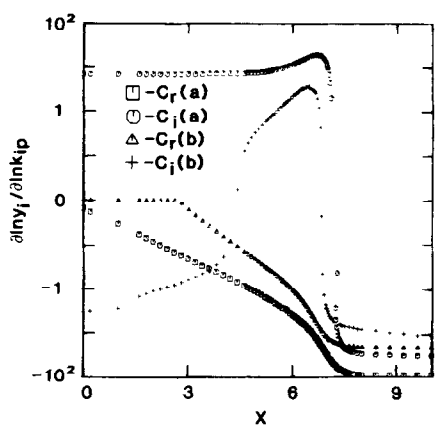

FIG. 9. Normalized first-order sensitivity coefficients of the reactant and the intermediate with respect to k_{ip} for the variable temperature model and $k_{ip} = 1.0 \times 10^2$. (a) Predetermined flame speed, (b) augmented system with the additional flame speed equation.

[1] In principle, any other acceptable parameter could have its identification altered but the flame speed is special due to its important physical significance.

TABLE II

Elementary and Derived Flame Speed Sensitivities

α	$\partial \ln M_0/\partial \ln \alpha$	$-\left(\frac{\partial \ln T/\partial \ln \alpha}{\partial \ln T/\partial \ln M_0}\right)^a$
k_{ri}	0.23007	0.23039
k_{ip}	0.23826	0.23859
Le_r	0.17810	0.17832
Le_i	0.09740	0.09755
E_{ri}	−4.03809	−4.04353
E_{ip}	−0.51692	−0.51762
h_r	7.09140	7.10075
h_i	−3.77922	−3.78443

[a] Evaluated at $x^* = 1.6$.

fixed temperature point does the indirect effect dominate and the sensitivity results become similar to those for the case in which the temperature value is not fixed.

The (elementary) sensitivity values of the flame speed with respect to the system parameters are given in Table II (the first column). Of course, since the flame speed does not have spatial dependence, its sensitivities are also constant. Similar to the sensitivities considered before, the flame speed is affected mainly by variations in the activation energies (which appear in the exponential terms of the model) and the specific enthalpies (due to the resulting temperature variations).

An additional demonstration of the different characteristics that arise with the fixed temperature point case is apparent from the results of the Green's function matrices presented in Fig. 10. These surfaces should be compared to the Green's surfaces for the original case shown in Fig. 4. We note the marked differences in the stability properties of the system in the region around the point at which the temperature is fixed. These differences are especially pronounced when the temperature is perturbed in this region. A response opposite to that shown in Fig. 4 is displayed by the species and the temperature. However, when the system is perturbed at a point further from the additional boundary point, the stability surfaces of the two cases are similar. The only differences occur in the region near the cold boundary where the system with the fixed temperature value is more stable.

VI. Derived Flame Speed Sensitivities

In the model considered originally, the flame speed M_0 appeared as a predetermined parameter of the system. By prescribing the temperature at an additional point x^* within the flame region, we were able to treat the flame speed as a dependent variable and, consequently, the sensitivity of the flame speed to variations of

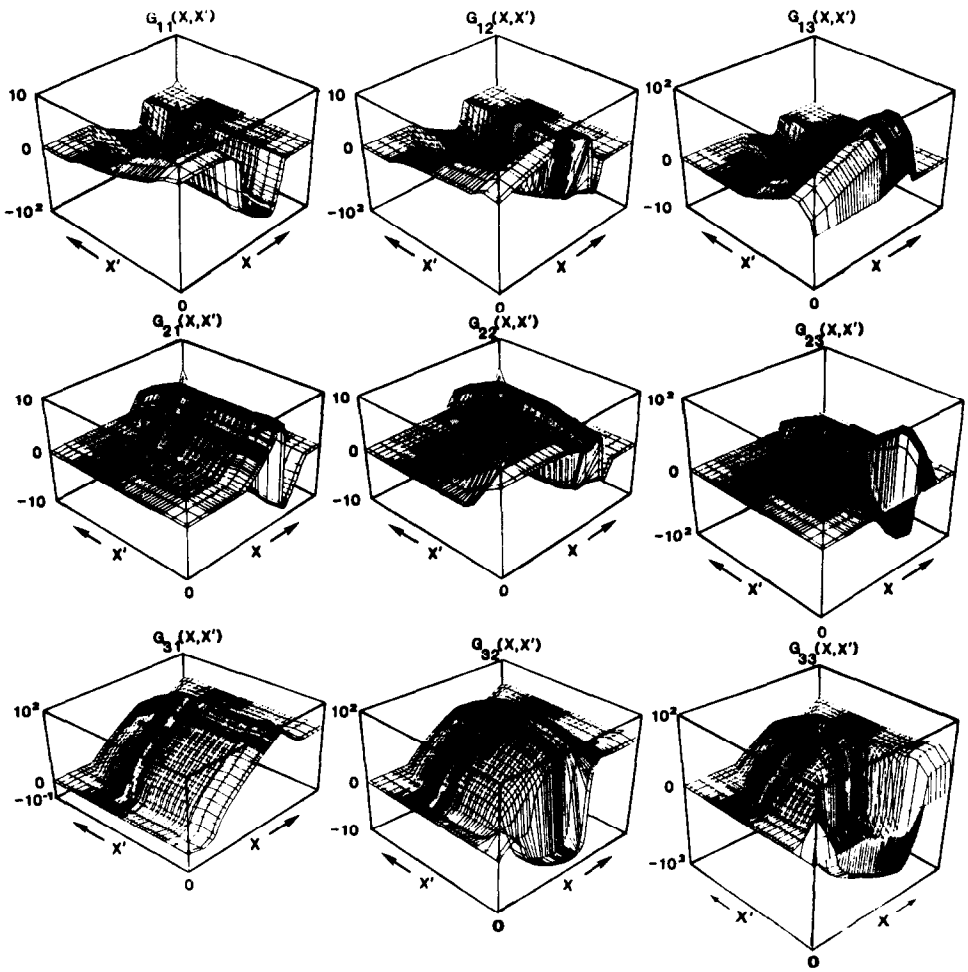

FIG. 10. The Green's function matrices for the variable temperature model with the additional flame speed equation and $k_{ip} = 1.0 \times 10^2$. The subscripts refer to (1) reactant, (2) intermediate, and (3) temperature. The vertical scales are logarithmic.

the system parameters was calculated. However, the transformation of the flame speed from a parameter to a dependent variable is exactly the process considered by derived sensitivities [3, 4, 7, 9, 10]. It has been shown that, when all the elementary sensitivities for a specific solution are available, it is possible to interchange a subset of dependent variables and parameters by using generalized Legendre transformations such that the sensitivities of these parameters with respect to the remaining parameters can be obtained. The connection between derived sensitivities and the operation of fixing a dependent variable (e.g., the temperature) at some point can

be understood by the following analysis. Consider the second-order, one-dimensional boundary value problem

$$L(y, \alpha) = 0, \qquad x_1 < x < x_2, \tag{6.1a}$$

$$y(x_1) = y^1, \tag{6.1b}$$

$$y(x_2) = y^2, \tag{6.1c}$$

and the analogous augmented system

$$L(y, \alpha) = 0, \qquad x_1 < x < x_2, \tag{6.2a}$$

$$\frac{d\alpha_1}{dx} = 0, \tag{6.2b}$$

$$y(x_1) = y^1, \tag{6.2c}$$

$$y(x_2) = y^2, \tag{6.2d}$$

$$y_1(x_3) = y_1^3, \qquad x_1 \leqslant x_3 \leqslant x_2. \tag{6.2e}$$

In the above equations y is the vector of N independent variables, α is the vector of M parameters, L is the differential operator and y^1, y^2 are the vectors of boundary values. In Eq. (6.2) one of the parameters, α_1, of Eq. (6.1) is treated as a dependent variable. Therefore, an explicit equation for α_1 is added and the value of one of the dependent variables, $y_1(x_3)$, *obtained from the solution of Eq.* (6.1), serves in (6.2) as the required additional boundary value. It is shown (see the Appendix) that the *same solutions* satisfy both the derived sensitivity equations for α_1 obtained from Eq. (6.1) by interchanging the role of α_1 and $y_1(x_3)$ and the elementary sensitivity equations obtained for α_1 from Eq. (6.2). Although this property for the derived sensitivities is demonstrated for a second-order Dirichlet problem, a generalization to any type of boundary condition and any order of equation can be made. The above similarity between derived and elementary sensitivities has more than mathematical importance. It can also give rise to additional physical interpretation of the derived sensitivities. In particular, one can look at the derived sensitivities for some parameter α_1 in a system of equations such as (6.1) as the elementary sensitivities for a similar system (6.2). In this system one of the dependent variables is predetermined at a point besides the boundaries and α_1 is turned into a dependent variable.

In the preceding section, the flame speed M_0 served as a parameter in the initial system of Eqs. (4.1)–(4.8), whereas its role was redefined to be a dependent variable in the last part of the section by adding Eq. (5.1). This replacement is entirely analogous to the passage from Eq. (6.1) to (6.2). Considering the flame speed sensitivities from a derived point of view with $T(x^*) = T^*$ leads to

$$\frac{\partial M_0}{\partial \alpha} = -(\partial T/\partial \alpha)/(\partial T/\partial M_0). \tag{6.3}$$

Numerical results for sensitivities of the flame speed with respect to several parameters obtained via equation (6.3) are presented in Table II (column 2). The good agreement between the results for the two sensitivity approaches serves not only as a numerical illustration of the mathematical proof in the Appendix, but also as an example of the numerical accuracy of the sensitivity results obtained by the two solution methods. An important issue concerning flame speed sensitivities is their possible dependence on the choice of T^* (and x^*) as an exchange variable. It was found numerically that $\partial M_0/\partial\alpha$ was not dependent appreciably on these choices—provided singular points (e.g., $\partial T(x^*)/\partial M_0 = 0$) were avoided.

VII. Summary and Conclusions

In this work a direct method for calculating the sensitivity coefficients and the Green's function matrices for boundary value problems was examined. The method takes advantage of the fact that the boundary value solver is based on a Newton iteration method. The Jacobian required for the Newton formula is, in principle, the same one that appears as the operator in the sensitivity equations. Thus the LU factored Jacobian used in the final step of the solution procedure can be used afterwards to calculate the sensitivity coefficients. As a result, considerable computational effort can be saved.

The usefulness of the sensitivity coefficients in the analysis of a model steady-state premixed flame based on a system of nonlinear, second-order, differential equations was demonstrated. The major physical outcome of the analysis was the prime importance of the temperature in determining the sensitivity behavior of the species in such a kinetic scheme. A better understanding of derived sensitivities was also achieved in this work. We illustrated that the derived sensitivities are, in fact, the elementary sensitivities of an augmented system with the relevant parameters as dependent variables and an equivalent number of former dependent variables fixed at a chosen spatial point.

We emphasize finally that the overall procedure of the modified Newton method plus sensitivity analysis represents a practical and accurate way of solving and assessing physically the behavior of nonlinear, coupled, two-point boundary value problems.

Appendix

In this Appendix, we illustrate that the derived sensitivities of a parameter α_1 in the boundary value problem (6.1) are equal to the elementary sensitivities for the same α_1 in the boundary value problem (6.2). To simplify the mathematical treatment, Dirichlet boundary conditions are chosen although the same proof can be generalized for more general boundary conditions.

A variation in the dependent variable vector as a result of parameter variations can be expressed generally as

$$dy = S\, d\alpha, \tag{A.1}$$

where dy is a differential change in the vector of N dependent variables as a result of a differential change $d\alpha$ in the vector of M parameters. The quantity S is the elementary sensitivities matrix with elements $S_{ij} = \partial y_i/\partial \alpha_j$. Suppose that one would like to interchange the role of one of the parameters, α_1, and one of the dependent variables, y_1, at some specific position, x_3, designated as y_1^3. This leads to the consideration of a new, derived sensitivity matrix S'. The structure of S' may be obtained by first rewriting Eq. (A.1) in the following manner

$$\begin{bmatrix} dy_1^3 \\ dy' \end{bmatrix} = \begin{bmatrix} S_1 & S_2 \\ S_3 & S_4 \end{bmatrix} \begin{bmatrix} d\alpha_1 \\ d\alpha' \end{bmatrix}. \tag{A.2}$$

In the above equation the vector dy' denotes the dependent variables at all the (discrete) positions except $y_1(x_3)$, the vector $d\alpha'$ represents all the parameters besides α_1, the term S_1 is the sensitivity element $\partial y_1^3/\partial \alpha_1$, the matrix S_2 is the row of sensitivities $\partial y_1^3/\partial \alpha'$, the matrix S_3 is the column of sensitivities $\partial y'/\partial \alpha_1$ and S_4 is the matrix of sensitivities $\partial y'/\partial \alpha'$. The equation for dy_1^3 can be written explicitly from Eq. (A.2) as

$$dy_1^3 = S_1\, d\alpha_1 + S_2\, d\alpha'. \tag{A.3}$$

Rearranging, we have

$$d\alpha_1 = S_1^{-1}\, dy_1^3 - S_1^{-1} S_2\, d\alpha', \tag{A.4}$$

where $S_1^{-1} = (\partial y_1^3/\partial \alpha_1)^{-1}$. Similarly, from Eq. (A.2) the equation for dy' is

$$dy' = S_3\, d\alpha_1 + S_4\, d\alpha', \tag{A.5}$$

and by substituting in Eq. (A.4) we obtain

$$dy' = S_3 S_1^{-1}\, dy_1^3 + (S_4 - S_3 S_1^{-1} S_2)\, d\alpha'. \tag{A.6}$$

From Eqs. (A.3)–(A.6) the equivalent blocks of the derived sensitivity matrix S' can be identified. We have

$$S_1' = S_1^{-1}, \tag{A.7}$$

$$S_2' = -S_1^{-1} S_2, \tag{A.8}$$

$$S_3' = S_3 S_1^{-1}, \tag{A.9}$$

$$S_4' = S_4 - S_3 S_1^{-1} S_2. \tag{A.10}$$

We now seek to show that the derived sensitivities coming from Eq. (6.1) are in fact the numerical solution to the elementary sensitivities of Eq. (6.2). We next differentiate (6.1) with respect to an arbitrary element α_j of the vector α so that we obtain the following system of sensitivity equations

$$J\frac{\partial y}{\partial \alpha_j} = -\frac{\partial L}{\partial \alpha_j}, \tag{A.11}$$

$$\frac{\partial y^1}{\partial \alpha_j} = \frac{\partial y^2}{\partial \alpha_j} = 0. \tag{A.12}$$

Here J is the Jacobian whose elements are $J_{ij} = \partial L_i/\partial y_j$. Similarly, if we write $\alpha \equiv (\alpha_1, \alpha')^{\mathrm{T}}$ as in (A.2) and then differentiate (6.2) with respect to every element α_j' of the vector α', we obtain

$$\frac{\partial L}{\partial \alpha_1}\frac{\partial \alpha_1}{\partial \alpha_j'} + J\frac{\partial y}{\partial \alpha_j'} = \frac{\partial L}{\partial \alpha_j'}, \tag{A.13}$$

$$\frac{d}{dx}\left(\frac{\partial \alpha_1}{\partial \alpha_j'}\right) = 0, \tag{A.14}$$

$$\frac{\partial y^1}{\partial \alpha_j'} = \frac{\partial y^2}{\partial \alpha_j'} = 0. \tag{A.15}$$

In Eq. (A.13) the derivative with respect to the additional boundary condition $\partial y_1^3/\partial \alpha_j' = 0$ is included in the vector $\partial y/\partial \alpha_j'$, such that the *same Jacobian* arises in equations (A.11)–(A.15).

The sensitivity equations with respect to the additional boundary condition y_1^3 are also obtained from Eq. (6.2),

$$\frac{\partial L}{\partial \alpha_1}\frac{\partial \alpha_1}{\partial y_1^3} + J\frac{\partial y}{\partial y_1^3} = 0, \tag{A.16}$$

$$\frac{d}{dx}\left(\frac{\partial \alpha_1}{\partial y_1^3}\right) = 0, \tag{A.17}$$

$$\frac{\partial y^1}{\partial y_1^3} = \frac{\partial y^2}{\partial y_1^3} = 0. \tag{A.18}$$

The extra boundary condition $\partial y_1^3/\partial y_1^3 = 1$ is included in the vector $\partial y/\partial y_1^3$. To complete the proof we first recognize that Eqs. (A.9)–(A.18) are differential equations. It is understood implicitly that they will be solved by a procedure similar to the one described in Sections II and III. In this case we recognize that S in Eq. (A.2) is the solution of equations (A.11), (A.12) and we will consider similarly the discretized solutions to Eqs. (A.13)–(A.18). One can show by appropriate matrix operations

and by using Eqs. (A.11) that the derived sensitivities in Eqs. (A.8) and (A.10) satisfy Eqs. (A.13), (A.14).

$$\frac{\partial L}{\partial \alpha_1} S_2' + JS_4' = \frac{\partial L}{\partial \alpha_j'}, \tag{A.19}$$

$$\frac{d}{dx} S_2' = 0. \tag{A.20}$$

The derivatives in equations (A.19)–(A.20) are understood to be treated by a discrete approximation. By applying the boundary conditions from Eq. (A.12) to Eq. (A.10), the boundary conditions in equations (A.14), (A.15) are also satisfied. In a similar way, it can be shown that the derived sensitivities (A.7) and (A.9) satisfy (A.16), (A.17). We have

$$\frac{\partial L}{\partial \alpha_1} S_1' + JS_3' = 0, \tag{A.21}$$

$$\frac{d}{dx} S_1' = 0. \tag{A.22}$$

The boundary conditions in Eq. (A.18) are satisfied by applying Eq. (A.12) to Eq. (A.9). This completes the proof.

REFERENCES

1. P. M. FRANK, "Introduction to System Sensitivity Theory," Academic Press, New York, 1978.
2. R. TOMOVIC AND M. VUKOBRATOVIC, "General Sensitivity Theory," Elsevier, New York, 1972.
3. H. RABITZ, *Comput. Chem.* **5** (1981), 167.
4. H. RABITZ, M. KRAMER AND D. DACOL, *Annu. Rev. Phys. Chem.* **34** (1983), 419.
5. J. W. TILDEN, V. COSTANZA, G. J. MCRAE, AND J. H. SEINFELD, *in* "Modeling of Chemical Reaction Systems" (K. H. Ebert, P. Deuflhard, and W. Jäger, Eds.), Springer Series in Chemical Physics, No. 18, Springer-Verlag, New York, 1981.
6. J. T. HWANG, E. P. DOUGHERTY, S. RABITZ, AND H. RABITZ, *J. Chem. Phys.* **69** (1978), 5180.
7. E. P. DOUGHERTY, J. T. HWANG, AND H. RABITZ, *J. Chem. Phys.* **71** (1979), 1794.
8. M. DEMIRALP AND H. RABITZ, *J. Chem. Phys.* **74**, (1981), 3362.
9. M. DEMIRALP AND H. RABITZ, *J. Chem. Phys.* **75**, (1981), 1810.
10. R. YETTER, L. A. ESLAVA, F. DRYER, AND H. RABITZ, *J. Phys. Chem.* **88**, (1984), 1497.
11. M. A. KRAMER, J. M. CALO, AND H. RABITZ, *Appl. Math. Model.* **5**, (1981), 432.
12. M. A. KRAMER, J. M. CALO, H. RABITZ, AND R. J. KEE, Sandia Tech. Rep. 82-9231, Livermore, Calif.
13. M. A. KRAMER, H. RABITZ, AND R. J. KEE, Sandia Tech. Rep. 82-8230, Livermore, Calif.
16. H. SAITO AND L. E. SCRIVEN, *J. Comput. Phys.* **42** (1981), 53.
17. C. L. IRWIN AND T. J. O'BRIEN, DOE/METC Tech Rep. 53, Morgantown, W. V.
18. B. LOJEK, *IEEE Proc.* **129G**, (1982), 85.

19. A. M. DUNKER, *Atmos. Environ.* **15**, (1981), 1155.
20. N. PETERS AND W. HOCKS, *in* "Gasdynamics and Chemical Lasers" (M. Firbig and H. Hügel, Eds.), DFVLR-Press, Germany, 1977.
21. V. S. BERMAN AND IU. S. RIZANTSEV, *J. Appl. Math. Mech.* **37**, (1973), 995.
22. A. K. KAPILA AND G. S. S. LUDFORD, *Combust Flame* **29**, (1977), 167.
23. G. JOULIN AND P. CLAVIN, *Combust. Flame* **25**, (1975), 389.
24. S. B. MARGOLIS, *Quart. Appl. Math.* **38**, (1980), 61.
25. M. D. SMOOKE, *J. Comput. Phys.* **48**, (1982), 72.
26. R. BULIRSCH, J. STOER, AND P. DEUFLHARD, "Numerical Solution of Nonlinear Two-Point Boundary Value Problems I," Numer. Math. Handbook Series Approximation, 1976.
27. V. PEREYRA, "PASVA3: An Adaptive Finite Difference Fortran Program for First Order Nonlinear, Ordinary Boundary Problems," Presented at the Conference for Working Codes for Boundary Value Problems in ODE's (B. Childs *et al.*, Eds.), Springer-Verlag, New York, 1979.
28. U. ASCHER, J. CHRISTIANSEN, AND R. D. RUSSELL, "COLSYS—A Collocation Code for Boundary Value Problems," Presented at the Conference for Working Codes for Boundary Value Problems in ODE's (B. Childs *et al.*, Eds.), Springer-Verlag, New York, 1979.
29. H. B. KELLER, "Numerical Methods for Two-point Boundary Value Problems," Blaisdell, Waltham, Mass., 1968.
30. M. L. SCOTT AND H. A. WATTS, *SIAM. J. Numer. Anal.* **14** (1977), 40.
31. M. D. SMOOKE, *J. Opt. Theory Appl.* **39**, (1983), 489.
32. V. PEREYRA AND E. G. SEWELL, *Numer. Math.* **23** (1975), 261.
33. A. B. WHITE, *SIAM J. Numer. Anal.* **16**, (1979), 472.
34. L. V. KANTOROVICH AND G. P. AKILOV, "Functional Analysis in Normed Spaces," Pergamon, Oxford, 1964.
35. M. D. SMOOKE, J. A. MILLER, AND R. J. KEE, *Combust. Sci. Technol.* **34**, (1983), 79.